



ELSEVIER

Journal of Biomechanics ■ (■■■■) ■■■-■■■

**JOURNAL
OF
BIOMECHANICS**

www.elsevier.com/locate/jbiomech
www.JBiomech.com

Methodology and sensitivity studies for finite element modeling of the inferior glenohumeral ligament complex

Benjamin J. Ellis^a, Richard E. Debski^b, Susan M. Moore^b,
Patrick J. McMahon^c, Jeffrey A. Weiss^{a,*}

^a*Departments of Bioengineering and Orthopedics, and Scientific Computing and Imaging Institute, University of Utah, Central Campus Drive, Rm. 2480, Salt Lake City, UT, USA*

^b*Musculoskeletal Research Center, Department of Bioengineering, University of Pittsburgh, Pittsburgh, PA, USA*

^c*Department of Orthopaedic Surgery, University of Pittsburgh, Pittsburgh, PA, USA*

Accepted 30 January 2006

Abstract

The objectives of this research were to develop a methodology for three-dimensional finite element (FE) modeling of the inferior glenohumeral ligament complex (IGHL complex) as a continuous structure, to determine optimal mesh density for FE simulations, to examine strains and forces in the IGHL complex in clinically relevant joint positions, and to perform sensitivity studies to assess the effects of assumed material properties. A simple translation test in the anterior direction was performed on a cadaveric shoulder, with the humerus oriented at 60° of glenohumeral abduction and 0° of flexion/extension, at 0°, 30° and 60° of humeral external rotation. The geometries of the relevant structures were extracted from volumetric CT data to create a FE model. Experimentally measured kinematics were applied to the FE model to simulate the simple translation test. First principal strains, insertion site forces and contact forces were analyzed. At maximum anterior humeral translation, strains in the IGHL complex were highly inhomogeneous for all external rotation angles. The motion of the humerus with respect to the glenoid during the simple translation test produced a tangential load at the proximal and distal edges of the IGHL complex. This loading was primarily in the plane of the inferior glenohumeral ligament complex, producing an in-plane shear-loading pattern. There was a significant increase in strain with increasing angle of external rotation. The largest insertion site forces occurred at the axillary pouch insertion to the humerus (36.7 N at 60° of external rotation) and the highest contact forces were between the anterior band of the IGHL complex and the humeral cartilage (7.3 N at 60° of external rotation). Strain predictions were highly sensitive to changes in the ratio of bulk to shear modulus of the IGHL complex, while predictions were moderately sensitive to changes in elastic modulus of the IGHL complex. Changes to the material properties of the humeral cartilage had little effect on predicted strains. The methodologies developed in this research and the results of the mesh convergence and sensitivity studies provide a basis for the subject-specific modeling of the mechanics of the IGHL complex.

© 2006 Elsevier Ltd. All rights reserved.

Keywords: Inferior glenohumeral ligament; Soft tissue mechanics; Strain; Finite element

1. Introduction

Nearly 2% of the population in the US will dislocate their glenohumeral (GH) joint. (Hovelius, 1982; Nelson

and Arciero, 2000). Eighty percent of these injuries will occur due to anterior dislocation of the humerus (Cave et al., 1974). The injuries include detachment of the inferior glenohumeral ligament complex (IGHL complex) from the anterior glenoid and labrum (Bankart, 1923, 1938) and humeral avulsion of the GH ligaments (Bokor et al., 1999; Bui-Mansfield et al., 2002; Chhabra et al., 2004; Richards and Burkhart, 2004; Sailer and Imhof, 2004; Schippinger et al., 2001; Warner and Beim,

*Corresponding author. Department of Bioengineering, University of Utah, Central Campus Drive, Rm. 2480, Salt Lake City, UT, USA. Tel.: +1 801 587 7833; fax: +1 801 585 5361.

E-mail address: jeff.weiss@utah.edu (J.A. Weiss).

1997). Initial and differential diagnosis of these injuries is often difficult due to the complex function of the GH capsule.

The specific contribution of regions of the IGHL complex to joint function has continued to be a source of controversy. GH capsule function has been examined via cutting studies (Turkel et al., 1981) and by evaluating the strains (Brenneke et al., 2000), elongation (Warner et al., 1993), in situ forces (Debski et al., 1999b), and material properties (Bigliani et al., 1992; Itoi et al., 1993; McMahon et al., 1998; Moore et al., 2004a; Ticker et al., 1996) of capsular regions. A recent study of strain in the antero-inferior capsule under subluxation demonstrated that maximum principal strains were highly variable (Malicky et al., 2001). Strain patterns did not correspond to any specific capsular region and instead encompassed several regions. Additionally, bi-directional material properties of the axillary pouch and posterior capsular regions have recently been evaluated (Moore et al., 2003, 2004a) and collagen fiber organization was quantified for several regions (Debski et al., 2003). Debski et al. (1999b) reported that significant forces were transmitted by the capsular regions, both between scapula and humerus and between capsular regions.

These and other studies support the notion that capsular regions experience multi-axial loading when subjected to joint kinematics that are representative of normal and injurious motions, and that the IGHL complex functions as a continuous structure (Debski et al., 2003, 1999b; Malicky et al., 2001; Moore et al., 2003, 2004a). However, previous computational models have represented the capsule as a collection of discrete one-dimensional structures (Debski et al., 1999a; Miller et al., 1991; Novotny et al., 2000). Similarly, computational models of the musculature at the GH joint have neglected the capsule due to its complex function (Luo et al., 1998; Novotny et al., 2000; Van der Helm, 1994a, b). A methodology to evaluate function of the capsule as a continuous structure would provide greater insight into the mechanical contribution of the IGHL to joint function, provide a means to identify joint positions that place the capsule at risk, identify potential improvements to surgical repair techniques, and provide a quantitative means for developing low-risk rehabilitation protocols.

The finite element (FE) method can represent the capsular regions as three-dimensional and continuous, providing predictions of strain, insertion site forces, and contact. However, there are a number of difficulties associated with FE modeling of the IGHL complex as a continuous structure. The geometry of both the bones and the capsule are complex and can vary appreciably between individuals (DePalma et al., 1949; Schwartz et al., 1988; Warner et al., 1993, 1992). IGHL material properties also exhibit variation between donors (Biglia-

ni et al., 1992; Itoi et al., 1993; McMahon et al., 1998; Moore et al., 2004a; Ticker et al., 1996). The capsule develops folds and creases during anatomical motion (Malicky et al., 2001), which presents difficulties for analysis with the FE method (Weiss et al., 2005). The establishment of a reference configuration for strain and stress measurement causes additional complications (Malicky et al., 2001). Finally, the appropriate mesh discretization needed to produce accurate predictions of capsular strains and insertion site forces, and the sensitivity of the continuum FE models to variations in model inputs are unknown. Previous efforts to model the IGHL complex have not addressed these issues (Debski et al., 1999a; Miller et al., 1991; Novotny et al., 2000).

The objective of this research was to develop a combined experimental-computational framework that can be used in the future for subject-specific FE modeling of the IGHL complex. The specific objectives of this study were (1) to develop an approach for FE representation of the IGHL complex as a continuous structure based on subject-specific geometry and discretization with shell elements, (2) to examine the patterns of IGHL strains, insertion site forces and contact forces during a simulated clinical examination, and (3) to test the sensitivity of the FE model to changes in IGHL complex and humeral articular cartilage material properties.

2. Materials and methods

2.1. Experimental kinematics

An intact shoulder (Male, 46 yrs) with no signs of arthritis or previous injury was used. After thawing for 12 h, the shoulder was dissected, leaving the humerus, scapula, rotator cuff tendons and capsule intact. The capsule was vented at the rotator cuff interval to allow insertion of compressed air during the CT scan. Plexiglas blocks and magnetic sensors were adhered to the scapula and humerus to allow definition of local coordinate systems for co-registration of kinematic and CT datasets. A load of 13.4 N was applied to each of the rotator cuff tendons (Debski et al., 1995). Using a magnetic tracking device (Flock of Birds, Ascension Technologies, Inc.), the Plexiglas blocks were digitized and local coordinate systems were established. Soft tissues were preconditioned to minimize viscoelastic effects by cycling the joint between the neutral position and maximum anterior and posterior translation. A clinician translated the humeral head to its limit in the anterior direction at 0°, 30°, and 60° of external rotation (ER) and 60° of abduction while joint kinematics were recorded. The reproducibility of this loading method and the accuracy of the measurements have been

published previously (Moore et al., 2004b). Accuracy of the magnetic sensors is $<0.3\%$ of the distance between the sensors and $<1.0^\circ$ (Moore et al., 2004b; Zeminski, 2001).

2.2. Reference strain state and volumetric CT scan

Rubber tubes (1/8" diameter) were used to facilitate visualization of the regions and insertion sites of the IGHL complex in the CT images (Fig. 1). Spherical nylon markers (6 × 6 grid, 1.6 mm diameter) were affixed to the regions of the IGHL complex. To establish a reference strain state, the joint was first positioned at 60° of GH abduction, 0° of horizontal abduction, and 15° of ER. The humerus was then internally rotated in 5° increments from 15° of ER to 15° of internal rotation, yielding seven joint positions. At each joint position, the capsule was inflated with compressed air to 0.7 and 4.8 kPa and photographs were taken at each pressure from two digital cameras. For each joint position, the images obtained from the digital cameras were superimposed. By visual inspection of the superimposed images, the joint position corresponding to the least marker movement between 0.7 and 4.8 kPa was determined (Malicky et al., 2001). With the joint in this position (60° abduction, 0° flexion, 45° ER), a volumetric CT scan was acquired (CTI; General Electric, Milwaukee, WI, USA). Thus, the folds and wrinkles of the capsule were minimized and the reference strain state was established. 191 CT slices were collected (slice thickness = 1 mm, FOV = 150 mm, in-plane resolution = 512×512).

2.3. Finite element mesh generation

Cross-sectional contours of the scapula, humerus, humeral articular cartilage and IGHL complex were extracted from the CT dataset (SurfDriver, Kailua, Hawaii). Polygonal surfaces were generated (Boissonnat, 1988) and the surfaces were smoothed (Schroeder

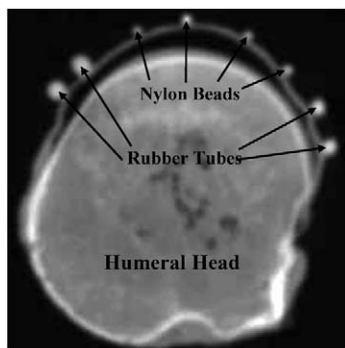


Fig. 1. CT image of the humeral head and IGHL complex. Rubber tubes and nylon beads mark the boundaries of the AB-IGHL, PB-IGHL, and axillary pouch.

et al., 1992). Polygons composing the surfaces of the scapula and humerus were converted directly to shell elements, which were used to represent the bones as rigid bodies (Ellis et al., 2006; Maker, 1995b). The IGHL complex and humeral cartilage surfaces were imported into FE preprocessing software (TrueGrid, XYZ Scientific, Livermore, CA, USA). A quadrilateral shell mesh was created for the IGHL, while a hexahedral mesh was created for the humeral cartilage (Debski et al., 2005) (Fig. 2). The initial mesh for the IGHL complex consisted of 5750 shells, while the cartilage mesh contained 7200 hexahedrons.

2.4. Material properties

The IGHL complex was represented as isotropic hypoelastic and the baseline modulus and Poisson's ratio ($E = 10.1$ MPa, $\nu = 0.4$) were obtained from a previous study (Moore et al., 2004a). Note that hypoelasticity is objective for finite deformations (i.e., large strains and rotations) (Simo and Hughes, 1998). The humeral head articular cartilage was represented as neo-Hookean hyperelastic (Maker et al., 1990) and the

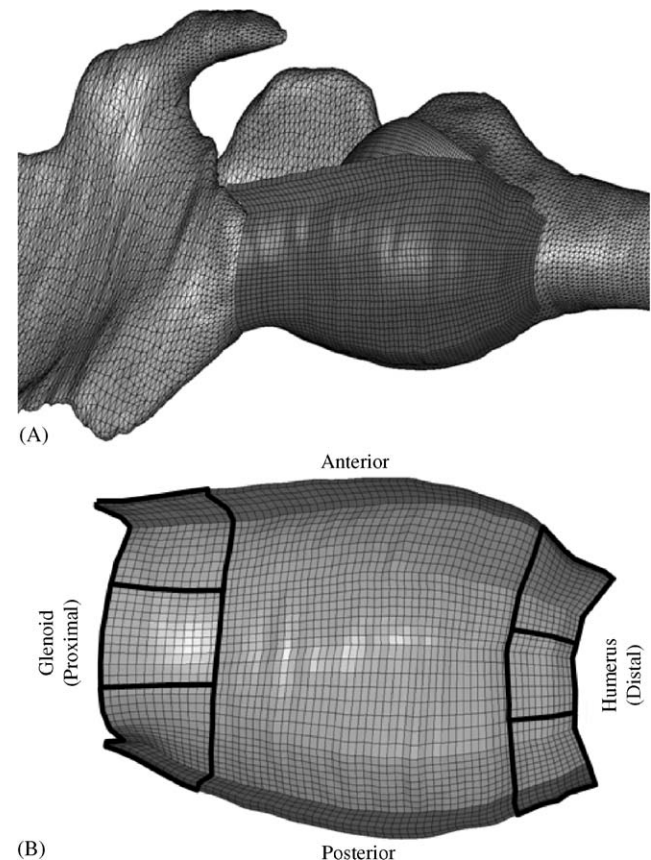


Fig. 2. (A) FE mesh of the IGHL complex, humerus, humeral cartilage, and scapula and (B) IGHL complex marked with the six strain regions (anterior distal, anterior proximal, middle distal, middle proximal, posterior distal, and posterior proximal) used for 1st principal strain analysis.

shear modulus ($C_1 = 0.3055$ MPa) was calculated from the modulus and Poisson's ratio ($E = 0.66$ MPa, $\nu = 0.08$) obtained from a previous study (Matsen and Hawkins, 1993). The scapula and humerus were modeled as rigid bodies.

2.5. Boundary conditions

The experimentally measured kinematic dataset was used to prescribe motion of the humerus (Ellis et al., 2006; Gardiner and Weiss, 2003). The coordinates of the Plexiglas blocks in both the CT and kinematic datasets allowed for correlation of the two datasets. Motion was described using incremental translations and rotations (Maker, 1995b; Simo and Vu-Quoc, 1988), based on the experimental measurements of the motion of the Plexiglas blocks on the humerus and scapula. Separate node sets were defined for the attachment of each IGHL region to each bone so that insertion site forces could be obtained for each region of the IGHL complex. Contact between capsular regions and the articular cartilage was enforced using the penalty method.

2.6. FE solution procedure

The nonlinear FE code NIKED was used for all analyses (Maker, 1995a). Nonlinear iterations were based on a quasi-Newton method and convergence was based on the L_2 displacement and energy norms. LSPOST (Livermore Software Technology Corporation, Livermore, CA, USA) was used to visualize and output strains while contact and insertion site forces were obtained directly from NIKED.

2.7. Regional strains, contact forces, and insertion site forces

To compare strains in regions of the IGHL complex, six areas were defined to represent the anterior distal, anterior proximal, middle distal, middle proximal, posterior distal, and posterior proximal regions (Fig. 2). Average 1st principal Green–Lagrange strains were calculated for each area. Insertion site forces and contact forces were also determined at the glenoid and humerus for the AB-IGHL, PB-IGHL and axillary pouch.

2.8. Mesh convergence study

To determine the mesh refinement level necessary to predict converged values of IGHL strains and forces, three additional FE models with mesh densities of twice, half, and a quarter the number of elements as the original mesh were analyzed.

2.9. Sensitivity studies

Studies were conducted to determine the sensitivity of FE predictions of IGHL strains and forces to assumed material properties. To assess the influence of elastic modulus on strains in the IGHL complex, the baseline modulus was increased and decreased by both 25% and 50%.

Baseline studies assumed a Poisson's ratio of $\nu = 0.4$, yielding a bulk:shear modulus ratio of 4.67. To assess the influence of the IGHL complex bulk:shear modulus ratio, three additional models were analyzed using bulk:shear modulus ratios of 1.0, 10.0, and 100.0 by maintaining the same elastic modulus and varying the Poisson's ratio.

Wrapping of the IGHL complex around the cartilage surface of the humeral head influences its deformation, but it is unclear whether the deformation of the cartilage itself influences the strain predictions for the IGHL complex. To test the effect of the cartilage bulk:shear modulus ratio on predicted IGHL strains and forces, three additional simulations were performed with cartilage bulk:shear modulus ratios of 1.0, 10.0, and 1000.0. Finally, one additional simulation was performed to test the effect of changing the cartilage from a deformable material to a rigid body.

3. Results

3.1. Baseline FE model

The IGHL complex was primarily subjected to shear in the plane of the IGHL during the simple translation test (Fig. 3). High strains developed in the anterior distal and posterior proximal portions of the IGHL complex. The motion of the humerus with respect to the glenoid produced a tangential load at the proximal and distal edges of the IGHL complex. This loading was primarily in plane with the IGHL complex, producing an in-plane shear-loading pattern. This pattern was modified and intensified by increased ER of the humerus, which increased IGHL wrapping around the humeral head. The IGHL complex experienced folding and creasing at all three ER angles. Average wall clock time for each FE simulation was about 2.5 h, using two processors of an SGI Origin 2000.

IGHL strains were highly non-uniform during FE simulations of simple translation at 0° , 30° , and 60° of ER (Fig. 3). Strains in the anterior distal region were $6.3 \pm 6.1\%$, $11.9 \pm 12.3\%$, and $11.5 \pm 11.1\%$, at 0° , 30° , and 60° , respectively. Strains in the posterior proximal region were $10.7 \pm 6.1\%$, $10.7 \pm 8.3\%$, and $10.4 \pm 8.4\%$, at 0° , 30° , and 60° , respectively. Strains in the anterior proximal region were $1.5 \pm 0.9\%$, $1.6 \pm 1.4\%$, and $1.7 \pm 1.4\%$, at 0° , 30° , and 60° , respectively. Strains in

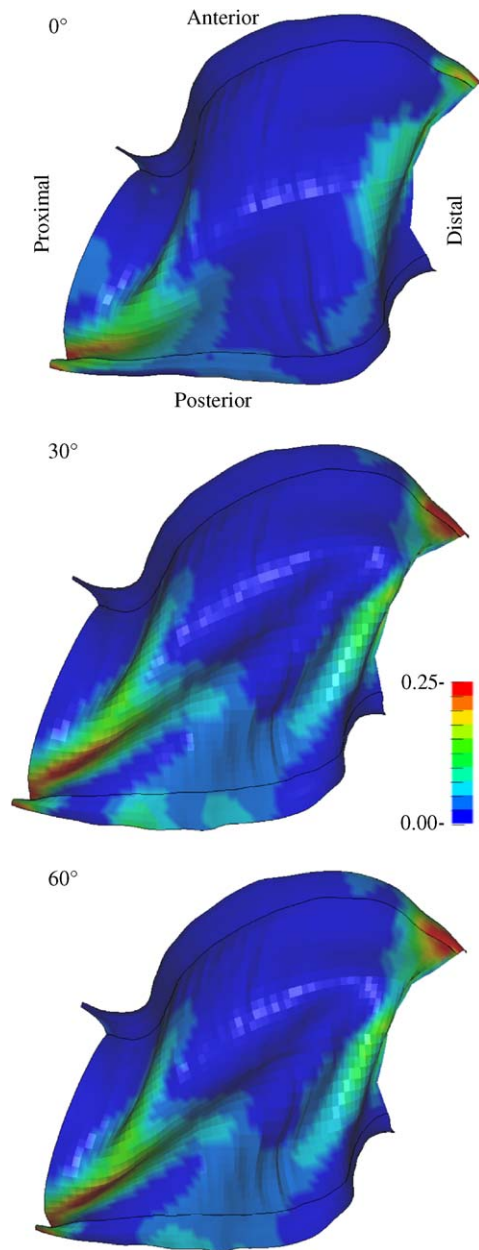


Fig. 3. Fringe plots of 1st principal strain at 60° of abduction and full anterior translations at 0°, 30°, and 60° of external rotation. Strains increased from 0° to 30° and from 0° to 60°, but there was little change in strains from 30° to 60°.

the posterior distal region were $1.0 \pm 1.1\%$, $2.1 \pm 2.0\%$, and $1.9 \pm 1.8\%$, at 0°, 30°, and 60° degrees, respectively (Fig. 4).

The highest insertion site forces occurred at the insertion of the axillary pouch to the humerus (25.8, 33.9, and 36.7 N, at 0°, 30°, and 60°, respectively) (Fig. 5). There were also relatively high forces at the axillary pouch insertion to the glenoid (16.8, 27.4, and 25.1 N, at 0°, 30°, and 60°, respectively). Insertion site forces at the AB-IGHL insertion to the humerus (16.8, 21.0, and 22.0 N, respectively) and the PB-IGHL

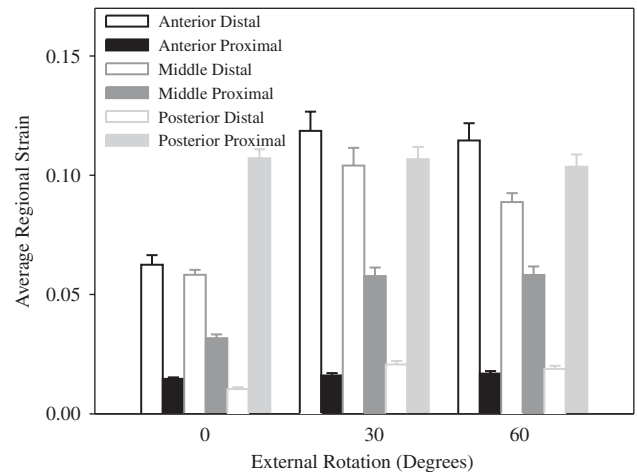


Fig. 4. 1st principal strain at 60° of abduction and full anterior translations at 0°, 30°, and 60° of external rotation. Strains in the anterior distal region and posterior proximal region were larger than strains in the other four regions.

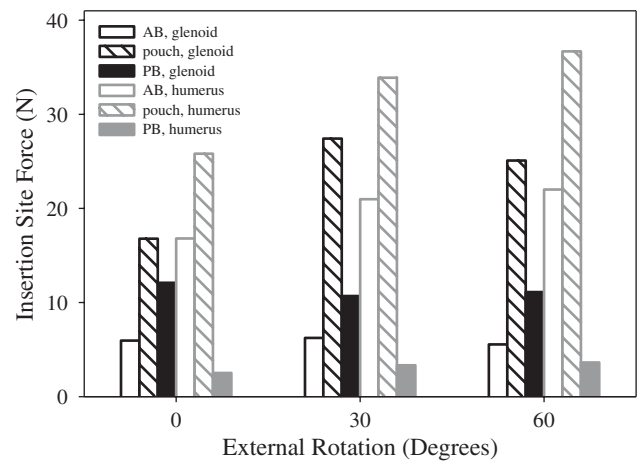


Fig. 5. Insertion site forces for the AB-IGHL, PB-IGHL, and axillary pouch at 60° of abduction and full anterior translations at 0°, 30°, and 60° of external rotation. The largest insertion site forces were consistently at the axillary pouch insertion to the humerus.

insertion to the glenoid (12.1, 10.7, and 11.1 N, respectively) were higher than the AB-IGHL insertion to the glenoid (6.0, 6.2, and 5.5 N, respectively) and the PB-IGHL insertion to the humerus (2.5, 3.3, and 3.6 N, respectively).

The highest contact forces occurred between the AB-IGHL and the humerus (5.2, 6.8, and 7.3 N, at 0°, 30°, and 60°, respectively). Contact forces between the axillary pouch and each bone were also relatively large (3.5 N at the humerus and 4.0 N at the glenoid, at 60°).

3.2. Mesh convergence study

Changes in mesh density had a large effect on strains, but little effect on forces. The mesh with twice as many

elements as the original mesh produced strains that on average were less than 1% different than the original mesh, but the mesh with a quarter as many elements produced strains that on average were 109% higher than the original mesh (Fig. 6). Meshes with twice as many elements and a quarter as many elements as the original mesh produced insertion site forces that on average were one percent less and five percent higher than the original mesh, respectively. Doubling the number of elements increased the average contact force by 2.4 N and the mesh with a quarter as many elements produced contact forces that were on average 0.96 N smaller than the original mesh. It was concluded that the original mesh provided a balance between accuracy and computational expense, and this FE mesh was used for the sensitivity studies.

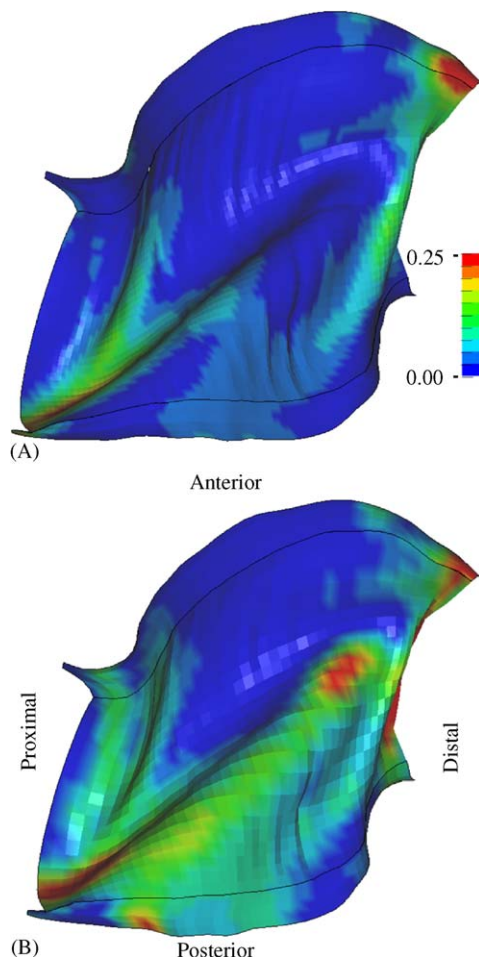


Fig. 6. Fringe plots of 1st principal strain at 60° of abduction and full anterior translations at 60° of external rotation for (A) the original mesh and (B) the mesh with a quarter as many elements as the original mesh. Do to the fact that large elements were bending around relatively tight folds, the mesh with a quarter as many elements produced 1st principal strains that were on average 109% higher than those for the original mesh.

3.3. Sensitivity to IGHL complex material properties

In general, there were small changes in strains with changes in elastic modulus of the IGHL complex. Average changes in strain over the six areas were 16%, -7%, -6%, and 14% with changes in the IGHL complex modulus of -50%, -25%, 25%, and 50%, respectively. The effect on the average change of the six insertion site forces with changes in the IGHL complex modulus was nearly linear (Fig. 7). The average changes in the insertion site forces were -46%, -26%, 31%, and 54% with changes in the IGHL complex modulus of -50%, -25%, 25%, and 50%, respectively. On average, there was less than a 2 N change in contact force.

Changes to the bulk:shear modulus ratio of the IGHL complex had a large effect on the strains and forces. Increasing the bulk:shear modulus ratio of the IGHL complex from 1.0 to 10.0 increased the average strains, insertion site and contact forces by 43%, 25%, and 470%, respectively. Increasing the IGHL complex bulk to shear modulus ratio from one to a hundred increased the average strains, insertion site and contact forces by 68%, 31%, and 100%, respectively.

3.4. Sensitivity to cartilage material properties

Changes to the elastic modulus and bulk:shear modulus ratio for the articular cartilage had little effect on predictions of strains and forces. There was less than a 1% change in average strains, a 1 N increase in average insertion site force, and less than a 1 N change in average contact force when the ratio of cartilage bulk:shear modulus was increased from 1.0 to 1000.0. Similarly, representing the cartilage as rigid decreased

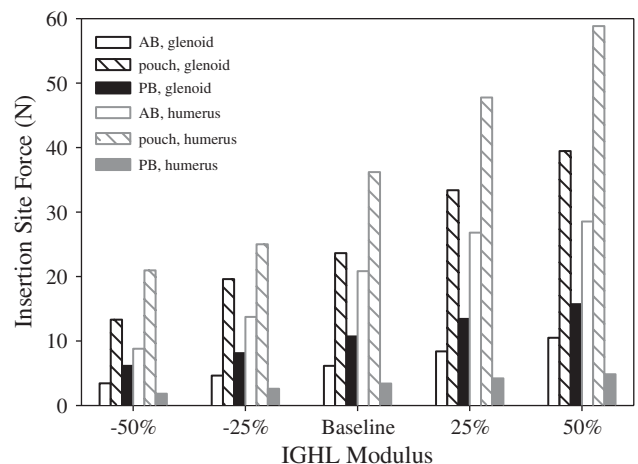


Fig. 7. Insertion site forces for the AB-IGHL, PB-IGHL, and axillary pouch at 60° of abduction and full anterior translations at 60° of external rotation for the baseline modulus, $\pm 25\%$ of baseline modulus, and $\pm 50\%$ of baseline modulus. The effect on the average change of the six insertion site forces with changes in the IGHL complex modulus was nearly linear.

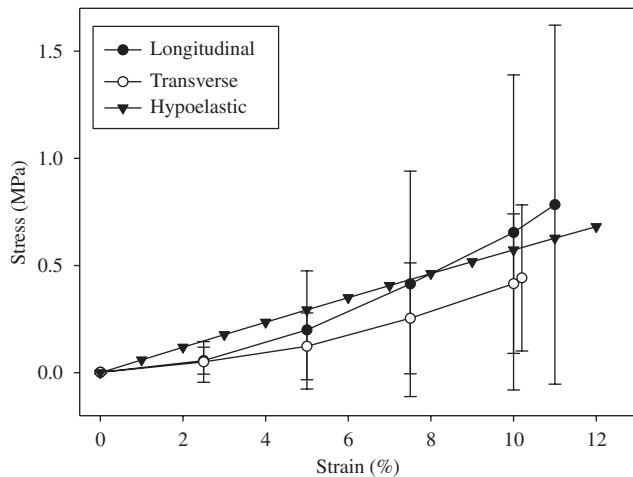


Fig. 8. Uniaxial tensile stress–strain response of the axillary pouch of the IGHL complex. Longitudinal—response parallel to the anterior band of the IGHL. Transverse—response transverse to the direction defined by the anterior band of the IGHL. Hypoelastic—material response of the hypoelastic constitutive model with best-fit material coefficients. Error bars are mean \pm standard deviation.

average strains by less than 1%, increased average insertion site forces by 2 N and decreased average contact force by less than 1 N.

4. Discussion

The FE models of the IGHL complex represented the three adjacent capsular regions as a continuous structure, using shell elements. This is in contrast with previous efforts that discretized the capsular regions with discrete one-dimensional elements (Debski et al., 1999a; Miller et al., 1991; Novotny et al., 2000). The ability to predict the three-dimensional strain distribution in the IGHL complex is a major advance of the current research over previous modeling efforts. Furthermore, the current model includes the wrapping of capsular tissue around the humeral head. Capsular wrapping has been previously described in ER (O'Brien et al., 1990), where the IGHL complex is the primary static restraint (Turkel et al., 1981). Thus, capsular wrapping may play a role in force transmission from the humerus to the glenoid, providing additional joint stability.

This study used quadrilateral shell elements to represent the IGHL complex (Hughes and Liu, 1981a, b). Our previous studies of ligament mechanics (Ellis et al., 2006; Gardiner and Weiss, 2003) have demonstrated that difficulties can arise when using hexahedral elements to represent ligaments that experience folding and creasing. In our previous study of the anterior band of the IGHL complex (Debski et al., 2005), we were successful in obtaining converged

solutions using hexahedral elements. However, when attempting to simulate the entire IGHL complex in the present study, hexahedral elements failed to yield converged solutions due to element inversion at the locations of developing folds. In fact, three different hexahedral element formulations were applied unsuccessfully to the simulations in this study (Puso, 2000; Simo and Armero, 1993; Simo and Taylor, 1991). Modeling the IGHL with shell elements also reduced computational expense. Not only do shell elements have fewer degrees of freedom than trilinear hexahedral elements, but only a single element is required to describe variations in strain through the thickness of the IGHL complex.

Strain predictions were much more sensitive than the forces to changes in mesh density. The sensitivity of the strains to mesh density was caused by folding of the IGHL complex. The use of fewer elements caused the (larger) shell elements to bend around relatively tight folds in the IGHL complex. Thus, models with a quarter and half as many elements produced higher strains than the original mesh and the mesh with twice as many elements (Fig. 6). In contrast, because the kinematics of the simple translation test subjected the IGHL complex to primarily in-plane shear loading, the forces were not sensitive to mesh density.

The sensitivity of FE predictions to changes in the IGHL complex material properties has important implications for future modeling efforts. Subject specific material properties may be needed to obtain accurate predictions of strain and force when future studies examine a population of subject-specific models for the IGHL complex. In contrast, the articular cartilage of the humeral head may be represented as rigid, decreasing the computational demand of future analyses. The strong tie between assumed material properties and predicted strains and forces, along with the high variation of IGHL complex material properties seen in experimental studies (Bigliani et al., 1992; Itoi et al., 1993; McMahon et al., 1998; Moore et al., 2004a; Ticker et al., 1996), suggests that there will also be a high variation in IGHL complex strains and forces in a population of specimens.

IGHL strains, insertion site and contact forces were all sensitive to changes in the IGHL bulk:shear modulus ratio. This is an important finding because there are little data available in the literature about the bulk (volumetric) behavior of ligaments in general. An experimental study to characterize the bulk behavior of the IGHL would help to eliminate the uncertainty associated with this parameter.

In contrast to the effects of IGHL complex material properties, IGHL complex strains and forces were insensitive to changes in articular cartilage elastic modulus and bulk:shear modulus ratio. This finding has implications for future IGHL modeling. Experiments

will not be needed to characterize the material properties of the humeral articular cartilage in order to produce accurate subject-specific models of the IGHL complex. This will lead to a reduction in the time needed for model construction because a hexahedral mesh will not be needed for the cartilage. Instead, the surface of the humeral articular cartilage can be generated as part of the humerus, converted directly to shell elements, and represented as a composite rigid body. Modeling the humeral articular cartilage as a rigid body saves computational expense in two ways. First, simulations of contact between a deformable body and a rigid body are computationally less expensive than simulations of contact between two deformable bodies. Second, representing cartilage as a rigid body directly saves computational time by removing the thousands of degrees of freedom introduced by a deformable hexahedral mesh.

To provide a framework for FE analysis in the absence of available experimental data, several assumptions regarding material behavior of the IGHL complex were made. First, a hypoelastic constitutive framework was used in the FE analyses. Although hypoelasticity is objective for large strains and rotations (Simo and Hughes, 1998), it neglects the upward-concave material behavior of the IGHL (Moore et al., 2003, 2004a). This assumption was justified based on data on the material behavior of the axillary pouch and anterior band of the IGHL complex (Moore et al., 2005, 2003, 2004a). Fig. 8 illustrates the tensile response of the axillary pouch of the IGHL and the FE simulated tensile response, using hypoelasticity and the material coefficients fit to these data. The agreement is reasonable for the purposes of this study. Second, the IGHL complex was represented as isotropic. The average tensile material behavior of the IGHL is mildly anisotropic (Debski et al., 2003; Moore et al., 2005, 2004a). Further, the collagen fiber organization in the IGHL is quite random (Debski et al., 2003). Thus, isotropic material symmetry provided a reasonable starting point for baseline FE simulations of the IGHL complex.

Although this FE model was not directly validated with subject-specific experimental strains and/or forces, strain predictions are in reasonable agreement with data of previous studies that measured strain during tensile testing or functional loading experiments (Malicky et al., 2001; McMahon et al., 1998; Moore et al., 2004a; Stefko et al., 1997). Malicky et al. (2001) determined that the mean maximum principal strain in the anterior–inferior capsule was 14% during subluxation in the anterior direction. Additionally, failure strains for the axillary pouch and posterior capsule have reported to be as high as 33% (Moore et al., 2004a) and 23% (Moore et al., 2003), respectively for the midsubstance of the tissue. However, since specimen-specific validation was not performed, caution should be used in interpretation of the absolute values for predictions of

strains, insertion site and contact forces. Further experiments are needed to obtain subject-specific validation of predicted regional strains.

Acknowledgments

Financial support from the Whitaker Foundation (RG-99-0.76) and the National Institutes of Health (AR47369 and AR050218) is gratefully acknowledged.

References

- Bankart, A.S.B., 1923. Recurrent or habitual dislocation of the shoulder joint. *British Medical Journal* 2, 1132–1133.
- Bankart, A.S.B., 1938. The pathology and treatment of recurrent dislocation of the shoulder joint. *British Journal of Surgery* 26, 23–29.
- Bigliani, L.U., Pollock, R.G., Soslowky, L.J., Flatow, E.V., Pawluk, R.J., Mow, V.C., 1992. Tensile properties of the inferior glenohumeral ligament. *Journal of Orthopaedic Research* 10, 187–197.
- Boissonnat, J.D., 1988. Shape reconstruction from planar cross-sections. *Computer Vision, Graphics and Image Processing* 44, 1–29.
- Bokor, D.J., Conboy, V.B., Olson, C., 1999. Anterior instability of the glenohumeral joint with humeral avulsion of the glenohumeral ligament. A review of 41 cases. *Journal of Bone and Joint Surgery—British Volume* 81, 93–96.
- Brenneke, S.L., Reid, J., Ching, R.P., Wheeler, D.L., 2000. Glenohumeral kinematics and capsulo-ligamentous strain resulting from laxity exams. *Clinical Biomechanics (Bristol, Avon)* 15, 735–742.
- Bui-Mansfield, L.T., Taylor, D.C., Uhorchak, J.M., Tenuta, J.J., 2002. Humeral avulsions of the glenohumeral ligament: imaging features and a review of the literature. *American Journal of Roentgenology* 179, 649–655.
- Cave, E., Burke, J., Boyd, R., 1974. *Trauma Management*. Year Book Medical Publishers, Chicago, IL 437pp.
- Chhabra, A., Diduch, D.R., Anderson, M., 2004. Arthroscopic repair of a posterior humeral avulsion of the inferior glenohumeral ligament (HAGL) lesion. *Arthroscopy* 20 (Suppl. 2), 73–76.
- Debski, R.E., McMahon, P.J., Thompson, W.O., Warner, J.P.P., Woo, S.L.-Y., Fu, F.U., 1995. A new dynamic testing apparatus to study glenohumeral joint motion. *Journal of Biomechanics* 27, 869–874.
- Debski, R.E., Wong, E.K., Woo, S.L.-Y., Fu, F.H., Warner, J.J., 1999a. An analytical approach to determine the in situ forces in the glenohumeral ligaments. *Journal of Biomechanical Engineering* 121, 311–315.
- Debski, R.E., Wong, E.K., Woo, S.L.-Y., Sakane, M., Fu, F.H., Warner, J.J., 1999b. In situ force distribution in the glenohumeral joint capsule during anterior–posterior loading. *Journal of Orthopaedic Research* 17, 769–776.
- Debski, R.E., Moore, S.M., Mercer, J.L., Sacks, M.S., McMahon, P.J., 2003. The collagen fibers of the anteroinferior capsulolabrum have multiaxial orientation to resist shoulder dislocation. *Journal of Shoulder and Elbow Surgery* 12, 247–252.
- Debski, R.E., Weiss, J.A., Newman, W.J., Moore, S.M., McMahon, P.J., 2005. Stress and strain in the anterior band of the inferior glenohumeral ligament during a simulated clinical examination. *Journal of Shoulder and Elbow Surgery* 14, S24–S31.
- DePalma, A.F., Callery, G., Bennett, G.A., 1949. Variational anatomy and degenerative lesions of the shoulder joint. *American Academy*

- of Orthopaedic Surgery Instructional Course Lecture Series 6, 225–281.
- Ellis, B.J., Lujan, T.J., Dalton, M.S., Weiss, J.A., 2006. MCL insertion site and contact forces in the ACL-deficient knee. *Journal of Orthopaedic Research*, to appear (accepted 3 October 2005).
- Gardiner, J.C., Weiss, J.A., 2003. Subject-specific finite element analysis of the human medial collateral ligament during valgus knee loading. *Journal of Orthopaedic Research* 21, 1098–1106.
- Hovellius, L., 1982. Incidence of shoulder dislocation in Sweden. *Clinical Orthopaedics*, 127–131.
- Hughes, T.J., Liu, W.K., 1981a. Nonlinear finite element analysis of shells: part II. Three dimensional shells. *Computational Methods in Applied Mechanics* 27, 331–362.
- Hughes, T.J., Liu, W.K., 1981b. Nonlinear finite element analysis of shells: part I. Two dimensional shells. *Computational Methods in Applied Mechanics* 27, 167–181.
- Itoi, E., Grabowski, J.J., Morrey, B.F., An, K.N., 1993. Capsular properties of the shoulder. *Tohoku Journal of Experimental Medicine* 171, 203–210.
- Luo, Z.P., Hsu, H.C., Grabowski, J.J., Morrey, B.F., An, K.-N., 1998. Mechanical environment associated with rotator cuff tears. *Journal of Shoulder and Elbow Surgery* 7, 616–620.
- Maker, B.N., 1995a. NIKE3D: A nonlinear, implicit, three-dimensional finite element code for solid and structural mechanics. Lawrence Livermore Lab Technical Report UCRL-MA-105268.
- Maker, B.N., 1995b. Rigid bodies for metal forming analysis with NIKE3D. University of California, Lawrence Livermore Lab Report UCRL-JC-119862, 1–8.
- Maker, B.N., Ferencz, R.M., Hallquist, J.O., 1990. NIKE3D: A nonlinear, implicit, three-dimensional finite element code for solid and structural mechanics. Lawrence Livermore National Laboratory Technical Report UCRL-MA-105268.
- Malicky, D.M., Soslowky, L.J., Kuhn, J.E., Bey, M.J., Mouro, C.M., et al., 2001. Total strain fields of the antero-inferior shoulder capsule under subluxation: a stereoradiogrammetric study. *Journal of Biomechanical Engineering* 123, 425–431.
- Matsen, F.A., Fu, F.H., Hawkins, R.J., 1993. The Shoulder: a balance of mobility and stability: workshop, Vail, Colorado, September 1992. Presented at American Academy of Orthopedic Surgeons, Rosemount, IL.
- McMahon, P.J., Tibone, J.E., Cawley, P.W., Hamilton, C., Fechter, J.D., ElAttrache, N.S., Lee, T.Q., 1998. The anterior band of the inferior glenohumeral ligament: Biomechanical properties from tensile testing in the position of apprehension. *Journal of Shoulder and Elbow Surgery* 7, 467–471.
- Miller, M.S., McMahon, P.J., Bains, P.K., Klein, A.H., Fu, F.H., 1991. A mathematical and experimental model of length change in the inferior glenohumeral ligament in the late cocking phase of pitching. *Transactions of the Orthopaedic Research Society* 16, 609.
- Moore, S.M., McMahon, P.J., Debski, R.E., 2003. Bi-directional mechanical properties of the posterior region of the glenohumeral capsule. In: *Proceedings of the 2003 Summer Bioengineering Conference*. pp. 107–108.
- Moore, S.M., McMahon, P.J., Debski, R.E., 2004a. Bi-directional mechanical properties of the axillary pouch of the glenohumeral capsule: implications for modeling and surgical repair. *Journal of Biomechanical Engineering* 126, 284–288.
- Moore, S.M., Musahl, V., McMahon, P.J., Debski, R.E., 2004b. Multidirectional kinematics of the glenohumeral joint during simulated simple translation tests: impact on clinical diagnoses. *Journal of Orthopaedic Research* 22, 889–894.
- Moore, S.M., McMahon, P.J., Azemi, E., Debski, R.E., 2005. Bi-directional mechanical properties of the posterior region of the glenohumeral capsule. *Journal of Biomechanics* 38, 1365–1369.
- Nelson, B.J., Arciero, R.A., 2000. Arthroscopic management of glenohumeral instability. *American Journal of Sports Medicine* 28, 602–614.
- Novotny, J.E., Beynon, B.D., Nichols, C.E., 2000. Modeling the stability of the human glenohumeral joint during external rotation. *Journal of Biomechanics* 33, 345–354.
- O'Brien, S.J., Neves, M.C., Arnoczky, S.P., Rozbruch, S.R., Dicarlo, E.F., et al., 1990. The anatomy and histology of the inferior glenohumeral ligament complex of the shoulder. *American Journal of Sports Medicine* 18, 449–456.
- Puso, M.A., 2000. A highly efficient enhanced assumed strain physically stabilized hexahedral element. *International Journal for Numerical Methods in Engineering* 49, 1029–1064.
- Richards, D.P., Burkhart, S.S., 2004. Arthroscopic humeral avulsion of the glenohumeral ligaments (HAGL) repair. *Arthroscopy* 20 (Suppl. 2), 134–141.
- Sailer, J., Imhof, H., 2004. Shoulder instability. *Radiologe* 44, 578–590.
- Schippinger, G., Vasiliu, P.S., Fankhauser, F., Clement, H.G., 2001. HAGL lesion occurring after successful arthroscopic Bankart repair. *Arthroscopy* 17, 206–208.
- Schroeder, W.J., Zarge, J., Lorensen, W.E., 1992. Decimation of triangle meshes. *Computer Graphics (Proceedings of SIGGRAPH)* 26, 65–70.
- Schwartz, R.E., O'Brien, S.J., Warren, R.F., Torzilli, P.A., 1988. Capsular restraints to anterior-posterior motion of the abducted shoulder. A biomechanical study. *Orthopaedic Transactions* 12, 727.
- Simo, J.C., Armero, F., 1993. Improved versions of enhanced strain tri-linear elements for 3D finite deformation problems. *Computer Methods in Applied Mechanics and Engineering* 110, 359–386.
- Simo, J.C., Hughes, T.J.R., 1998. *Computational Inelasticity*. New York.
- Simo, J.C., Taylor, R.L., 1991. Quasi-incompressible finite elasticity in principal stretches: Continuum basis and numerical algorithms. *Computer Methods in Applied Mechanics and Engineering* 85, 273–310.
- Simo, J.C., Vu-Quoc, L., 1988. On the dynamics in space of rods undergoing large deformations—a geometrically exact approach. *Computer Methods In Applied Mechanics And Engineering* 66, 125–161.
- Stefko, J.M., Tibone, J.E., Cawley, P.W., ElAttrache, N.E., McMahon, P.J., 1997. Strain of the anterior band of the inferior glenohumeral ligament during capsule failure. *Journal of Shoulder and Elbow Surgery* 6, 473–479.
- Ticker, J.B., Bigliani, L.U., Soslowky, L.J., Pawluk, R.J., Flatow, E.L., Mow, V.C., 1996. Inferior glenohumeral ligament: geometric and strain-rate dependent properties. *Journal of Shoulder and Elbow Surgery* 5, 269–279.
- Turkel, S.J., Panio, M.W., Marshall, J.L., Girgis, F.G., 1981. Stabilizing mechanisms preventing anterior dislocation of the glenohumeral joint. *Journal of Bone and Joint Surgery—America* 63, 1208–1217.
- Van der Helm, F.C., 1994a. Analysis of the kinematic and dynamic behavior of the shoulder mechanism. *Journal of Biomechanics* 27, 527–550.
- Van der Helm, F.C., 1994b. A finite element musculoskeletal model of the shoulder mechanism. *Journal of Biomechanics* 27, 551–569.
- Warner, J.J., Beim, G.M., 1997. Combined Bankart and HAGL lesion associated with anterior shoulder instability. *Arthroscopy* 13, 749–752.
- Warner, J.J.P., Deng, X.H., Warren, R.F., Torzilli, P.A., 1992. Static capsuloligamentous restraints to superior-inferior translation of the glenohumeral joint. *American Journal of Sports Medicine* 20, 675–685.

- Warner, J.J.P., Caborn, D.N., Berger, R., Fu, F.H., Seel, M., 1993. Dynamic capsuloligamentous anatomy of the glenohumeral joint. *Journal of Shoulder and Elbow Surgery* 2, 115–133.
- Weiss, J.A., Gardiner, J.C., Ellis, B.J., Lujan, T.J., Phatak, N.S., 2005. Three-dimensional finite element modeling of ligaments: technical aspects. *Medical Engineering and Physics* 27, 845–861.
- Zeminski, J., 2001. Development of a Combined Analytical and Experimental Approach to Reproduce Knee Kinematics for the Evaluation of Anterior Cruciate Ligament Function. Master's Thesis, University of Pittsburgh, Pittsburgh.